

# Evaluation of mediastinoscopy for cranial mediastinal and tracheobronchial lymphadenectomy in canine cadavers

Erin A. Gibson DVM, DACVS (Small Animal) | Kelsey Brust DVM, DACVR | Michele A. Steffey DVM, DACVS (Small Animal) 

William R. Prichard Veterinary Medical Teaching Hospital, School of Veterinary Medicine, University of California-Davis, Davis, California, USA

Department of Surgical and Radiological Sciences, School of Veterinary Medicine, University of California-Davis, Davis, California, USA

## Correspondence

Erin A. Gibson, William R. Prichard Veterinary Medical Teaching Hospital, School of Veterinary Medicine, University of California-Davis, Davis, CA, USA.  
Email: [eagibson@vet.upenn.edu](mailto:eagibson@vet.upenn.edu)

## Present address

Erin A. Gibson, Department of Clinical Sciences and Advanced Medicine, University of Pennsylvania Matthew J. Ryan Veterinary Hospital, Philadelphia, Pennsylvania, USA.

## Funding information

UC Davis Center for Companion Animal Health, Grant/Award Number: 2021-13-F

## Abstract

**Objective:** To report technical feasibility and describe procedural details of a novel single incision minimally invasive approach to the mediastinum in cadaver dogs.

**Study design:** Cadaveric study.

**Animals:** Large breed (25–40 kg) cadaver dogs ( $n = 10$ ).

**Methods:** Three of 10 cadavers were used for preliminary technique development without data recording. Cadaver specimens underwent pre- and postoperative thoracic computed tomographic scans. Seven dogs were placed in dorsal recumbency and mediastinoscopy was performed via a SILS port placed cranial to the thoracic inlet with CO<sub>2</sub> insufflation of the mediastinum at 2–4 mmHg. Retrieval of all CT and visually identified mediastinal lymph nodes (LN) was attempted; endoscopic compartmental and individual LN dissection times and subjective operative challenges were recorded. Procedural success scores for visualization and dissection as well as NASA-task force index scores were recorded per lymph node, per cadaver.

**Results:** Median time required for initial approach including SILS placement was 5 min (range 5–10 min). Individual LN retrieval times ranged from 2 to 32 min. Mediastinoscopic retrieval of LNs was most commonly successful for the left tracheobronchial LN (7/7), followed by the right tracheobronchial LN (4/7), the left and right sternal LNs (3/7 each), and the cranial mediastinal LNs (1/7). Post-procedure pleural gas was identified on CT in 4/7 cadavers.

**Conclusions:** Mediastinoscopy as reported was feasible in large breed canine cadavers and retrieval or cup biopsy of a variety of lymph nodes is possible from the described approach. Application in living animals and its associated challenges should be further investigated.

**Clinical significance:** Mediastinoscopy may provide a novel minimally invasive approach to the evaluation and oncologic staging of the cranial mediastinum in dogs.

This is an open access article under the terms of the [Creative Commons Attribution-NonCommercial-NoDerivs](https://creativecommons.org/licenses/by-nc-nd/4.0/) License, which permits use and distribution in any medium, provided the original work is properly cited, the use is non-commercial and no modifications or adaptations are made.

© 2024 The Authors. *Veterinary Surgery* published by Wiley Periodicals LLC on behalf of American College of Veterinary Surgeons.

## 1 | INTRODUCTION

The cranial mediastinum is a potential intrathoracic space cranial to the heart, containing structures such as regional lymph node centers, trachea, esophagus, great vessels, and nerves. Mediastinal diseases include primary neoplasia such as lymphoma, thymoma, heart-based tumors, ectopic thyroid carcinoma, and rarely sarcomas.<sup>1–3</sup> Metastatic disease secondary to primary pulmonary neoplasms is also represented within the mediastinum, specifically within the tracheobronchial and mediastinal lymph node stations. The most common primary lung tumor in dogs is pulmonary adenocarcinoma.<sup>4</sup> In dogs with lung carcinoma, stage 1 dogs treated with surgery have prolonged survival and delayed progression of disease, while these outcome measures are reduced with progressive stages.<sup>5–10</sup> As such, staging of intrathoracic lymph nodes would be helpful in treatment recommendations and prognosis, although challenges in staging thoracic lymph nodes include their small size, accessibility, and proximity to important neurovascular structures.<sup>11–14</sup>

Video-assisted mediastinoscopic lymphadenectomy (VAMLA) is a well-established diagnostic technique in diseases of the mediastinum in human medicine,<sup>15–21</sup> including oncologic staging of intrathoracic lymph nodes where cytologic or histologic sampling by less invasive methods is not possible, or where initial attempts fail to generate a diagnostic sample. This technique is used commonly for staging of non-small cell lung cancer in people.<sup>22,23</sup> Intrathoracic lymph node clusters are grouped into 14 stations, which are important prognostically in the setting of lung cancer.<sup>24,25</sup> Mediastinoscopy may reliably access three to five of the 14 stations, although additional stations may be accessed with standard or extended mediastinoscopy, anatomy allowing.<sup>19,23</sup> VAMLA has reported sensitivity and specificity rates for positive lymph node identification of 93%–100% and 94%–100%, respectively.<sup>20,21</sup>

The aim of this study was to assess anatomic feasibility of a novel VAMLA approach in canine cadavers, and to provide baseline data that would facilitate future clinical application in live dogs. Given the anatomic differences between humans and dogs, necessary procedure modifications for mediastinoscopic lymphadenectomy in dogs were anticipated. Feasibility was defined as the summed data collected in cadaveric specimens including cranial mediastinum dissection times, lymph node extirpation times, study-defined procedure success scoring for visualization and dissection, modified operative adverse events,<sup>26</sup> and technique difficulty reported via NASA-TLX.<sup>27,28</sup> Pre- and post-procedural thoracic CT was utilized to identify essential cranial mediastinal

structures and to identify procedural consequences that might represent clinically relevant post-procedural complications in future technique applications to living dogs.

## 2 | MATERIALS AND METHODS

The institutional animal care and use committee declined to evaluate this protocol due to the cadaveric nature of the study.

### 2.1 | Animals

Ten large breed (>20 kg) canine cadavers, previously humanely euthanized for reasons unrelated to participation in this study, were purchased from a commercial vendor (Skulls Unlimited, Oklahoma City, Oklahoma) for the purposes of this study. Prior to use, the cadavers were thawed over the span of 48 h.

### 2.2 | Thoracic imaging

Thoracic computed tomography (CT) scans were performed immediately prior to use in all thawed cadavers. CT was performed with a Lightspeed 16 helical scanner (General Electric Co, Milwaukee, Wisconsin) with acquisition parameters of 120 kVp, 200 mA, and 0.625 mm image thickness in a soft tissue algorithm. Prior to initiation of mediastinoscopy, specific anatomic structures including cranial mediastinal and tracheobronchial lymph nodes, esophagus, pulmonary trunk, carina, azygous vein, recurrent laryngeal nerve, aortic arch, internal thoracic vessels, thymus gland, and lateral pleural folds were noted or measured and recorded if identified on CT scans. Images were reviewed at a DICOM workstation with viewing software (AGFA workstations, Carlstadt, New Jersey) by a single board-certified radiologist (KB). Presence of pleural or mediastinal gas prior to the procedure was noted. The mediastinal space was further defined by the selected measurements of three regions based on CT scan. The site of maximal thymic diameter was determined and subsequently, the cross-sectional area of the cranial mediastinum at this point was determined in cm<sup>2</sup> and reported as a percentage of total thoracic cavity area at that site. This was repeated for each cadaver. The midpoint of the cranial mediastinum was selected as the midpoint from thoracic inlet to the heart, and volume of this area reported in the transverse plane as the product in centimeters of measured height and width. Distance from the thoracic inlet to the midpoint of the cranial mediastinum was reported in centimeters.

Cranial mediastinal and tracheobronchial lymph node width, height, and length were recorded as the widest linear measurement in each assigned direction, and lymph node volume calculated. Following mediastinoscopy, all cadaver specimens underwent a second thoracic CT and preprocedure structures were evaluated for their presence or absence to confirm that any structures removed had been correctly identified intraoperatively, and the presence of pleural, subcutaneous, and mediastinal gas was noted. Mediastinal gas was recorded as a percentage of total surface area at two pre-determined axial slices within the cranial mediastinum. The two pre-determined points were the site between the second and third ribs and the site between the manubrium and second sternal segment (Figure 1A). Pleural gas was reported as a percentage of total thoracic cavity area at the level of the mid-heart. The circumferential limits of subcutaneous and intermuscular gas, defined as the presence of gas within and expanding the normal intermuscular fissures, were described relative to the primary surgical site (thoracic inlet).

### 2.3 | Relevant anatomy

For the purposes of designing methodical surgical exploration, the cranial mediastinum was divided into a ventral and dorsal compartment, as illustrated in Figure 1B.

### 2.4 | Preliminary technique development

#### 2.4.1 | Standard VAMLA

A canine cadaver was placed in dorsal recumbency, with the ventral neck and cranial ventrolateral aspects of the thorax clipped fully. The neck was hyperextended (Figure 2A,B) to facilitate access to the thoracic inlet. The manubrium was palpated and the space ventral to the trachea and dorsal to the sternum identified. A linear longitudinal incision on midline (3–5 cm) was made within this space, and the skin, subcutaneous tissues, and cervical musculature divided to the level of the thoracic inlet with sharp dissection. A mediastinoscope (Karl Storz 10 972 SPS Linder/Hurtgen distending video mediastinoscope, Karl Storz, El Segundo, California) (Appendix Figure A1A,B) was placed within the incision along the ventral aspect of the trachea. The blades were hinged open as per the manufacturer's instructions in order to improve visualization of the mediastinum. Various mediastinoscope-specific instruments (Appendix Figure A1C,D) as well as standard

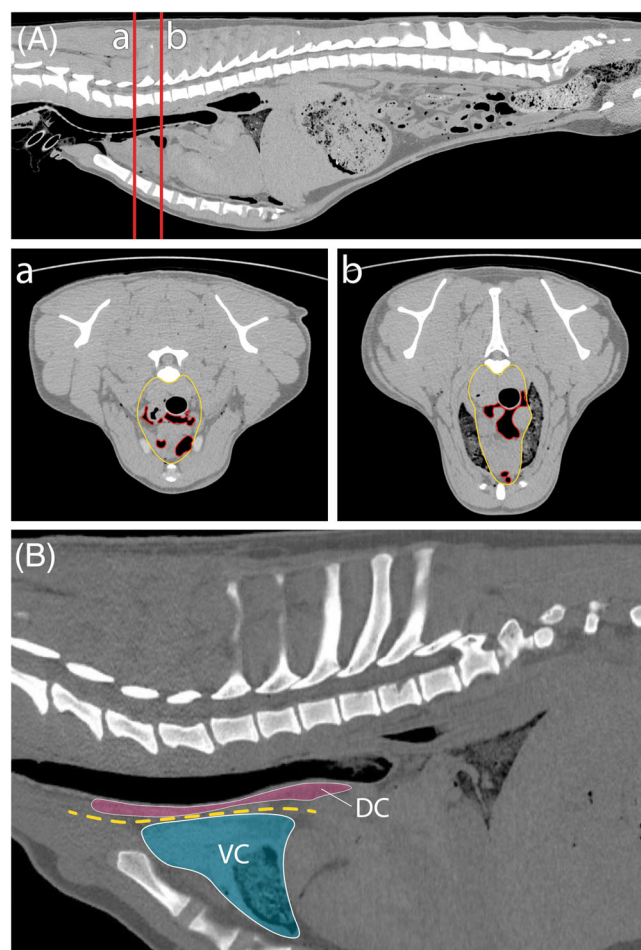


**FIGURE 1** Computed tomography (CT) assessments. (A) Sagittal image of thorax with red lines denoting the two pre-determined axial assessment within the cranial mediastinum. (a) denotes the cranial marker at a location between the second and third ribs and the corresponding the axial view at this location; (b) denotes the caudal marker at a location between the manubrium and second sternal segment and the corresponding axial view at this location. The mediastinal border is defined by the yellow outline and the red border outlines the free mediastinal gas quantified at these sections. (B) Sagittal image of CT scan of canine cadaver; blue shadowed compartment represents the ventral compartment, the yellow dotted line represents the division, and the pink shadowed section represents the potential space of the dorsal compartment.

laparoscopic instruments were passed through the open end of the mediastinoscope in order to attempt dissection of the ventral and dorsal compartments.

#### 2.4.2 | Alternative-VAMLA technique

Dogs were prepared and positioned as described for the standard-VAMLA technique, and superficial dissection was performed as described for VAMLA.

Following division of cervical musculature to access the thoracic inlet space, a blunt trocar was gently passed, hand-guided, into this potential space along the ventral aspect of the trachea (Figure 2C) and the paratracheal fascia and associated structures gently elevated. Following this, the SILS port (SILS Port, Medtronic, Watford, UK) was subsequently placed such that the cuff of the port was stabilized laterally by the paired bellies of the sternohyoideus muscle, and the port was in close apposition to the trachea, deep to the cervical musculature and paratracheal fascia (Figure 2D). Three

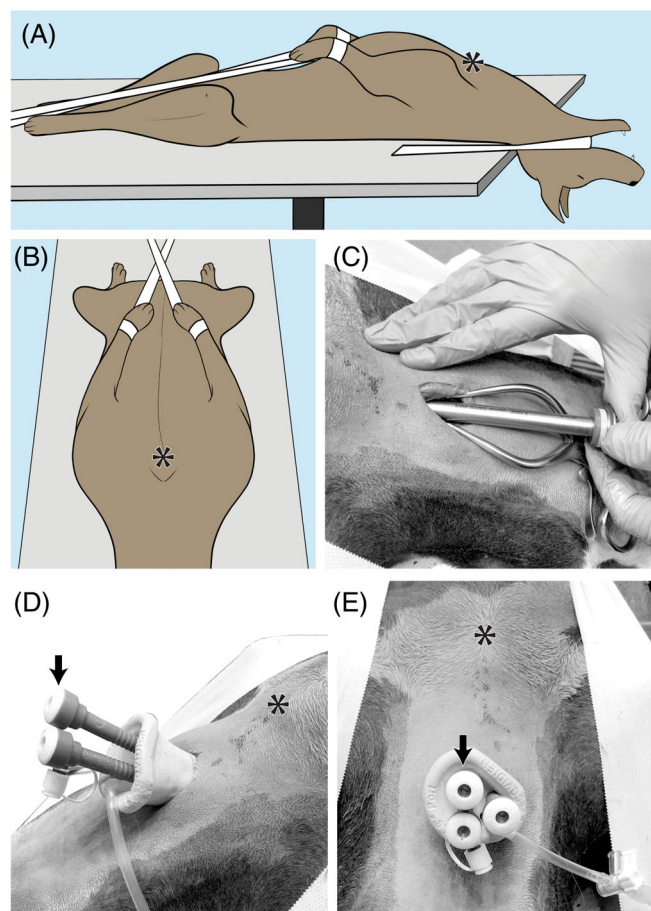


**FIGURE 2** Mediastinoscopy approach. (A) Demonstration of the positioning of cadaveric specimens during the mediastinoscopy approach and procedure. The dog's manubrium (an important surgical landmark) is identified by the asterisk. (B) Surgeon's view of the cadaver in position (asterisk identifies the manubrium). (C) Surgical approach to the thoracic inlet. Superficial retraction is maintained by gelpi retractors. Once the paratracheal fascia is reached, a blunt probe was used to aid in extension of the dissection plane into the mediastinum and avoid sharp trauma to nearby vascular structures while maintaining the limited approach window; Side view (D) and surgeon's view (E) of the SILS port in place at the thoracic inlet. The optimal position of the camera port is identified by the arrow. The manubrium is identified by an asterisk.

5 mm cannulas were passed into the SILS (Figure 2E), and insufflation applied at a pressure of 2–4 mmHg to generate pneumomediastinum using a mechanical insufflator (PneumoClear Insufflator, Stryker, Kalamazoo, Michigan). A 30-degree 5.4 mm endoscope (1588 AIM laparoscope, Stryker) was passed into one of the ports, and laparoscopic Kelly forceps and right-angle dissecting forceps were introduced through the remaining ports to perform mediastinal dissection to the level of the tracheal carina (Figure 3A,B). Following this, the left and right tracheobronchial lymph nodes were identified and dissected free of attachments with a combination of blunt dissection and a vessel sealing device (LigaSure Dolphin Tip Laparoscopic Sealer/Divider,

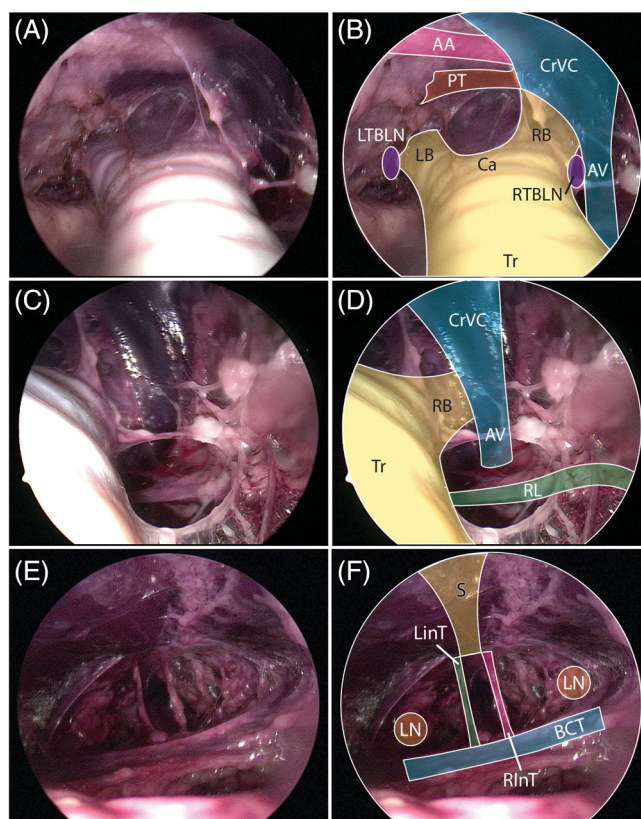


**FIGURE 3** Mediastinoscopic views within the dorsal and ventral compartments. Dorsal compartment, view of the carina (A) with corresponding labeled image (B) and focused view of the right bronchial area (C) with corresponding labeled image (D). AA, aortic arch; AV, azygos vein; CA, carina; CrVC, cranial vena cava; LB, left bronchus; LTBLN, left tracheobronchial lymph node; PT, pulmonary trunk; RB, right bronchus; RL, recurrent laryngeal nerve; RTBLN, right tracheobronchial lymph node; TR, trachea. Ventral compartment, mediastinoscopic view (E) with corresponding labeled image (F). BCT, brachiocephalic trunk; LInT, left internal thoracic vessel; LN, location of the right and left sternal lymph nodes; RInT, right internal thoracic vessel; S, sternum.

ValleyLab FT10 Energy Platform, Medtronic, Minneapolis, Minnesota) (Figure 3A–D).

Subsequently, the endoscope and instrumentation were retracted cranially to the cranial edge of the brachiocephalic trunk and oriented ventrally to access the ventral compartment (Figure 3E,F). The compartment was investigated for sternal and cranial mediastinal lymph nodes and when identified, the nodes were subsequently retrieved. The duration of time to complete exploration per compartment was recorded, and time to complete lymph node dissection was recorded per node.

All procedures were performed by a single board-certified surgeon with specialty training in minimally invasive surgery, under the direct supervision of a board-certified surgeon and ACVS Founding Fellow of Minimally Invasive Surgery. A modified version of the Operative Adverse Events Scale<sup>26</sup> was defined (Appendix S2), and any noted events were recorded. A mediastinal fat scoring system was developed for the purpose of this study based on mediastinoscopic view (Appendix S2). Scores were assigned per cadaver and recorded.

### 2.4.3 | Procedural success grading

A grading scheme was developed and utilized, ranging from 1 (optimal) to 5 (unachievable) for visualization of targeted structures within the dorsal and ventral compartments. A similar grading scheme ranging from 1 (optimal) to 5 (unachievable) for dissection and tissue extirpation of all lymph nodes visualized was also utilized (Appendix S2).

### 2.4.4 | Procedural difficulty

NASA-TLX (task load index, Appendix S2)<sup>27,28</sup> was completed for each subsection of the mediastinoscopy procedure following completion, including the exploration and dissection of the ventral compartment and dorsal compartment within the mediastinum, as well as for each retrieval of identified lymph nodes.

## 3 | RESULTS

Cadavers –ten mixed breed canine cadavers weighed a median of 27.5 kg (range 23.5–38.5 kg). Body condition score was a median of 5 (range 4–9) and mediastinal fat score was a median of 4 (range 3–4). Frozen cadavers were left at room temperature for 48–72 h until tissues were appropriately thawed to permit manipulation and dissection.

## 3.1 | Surgical technique development

Standard VAMLA (sVAMLA) – SVAMLA with a commercial mediastinoscope was attempted in the first cadaver. Attempts were made utilizing this mediastinoscope and associated purpose-specific instrumentation as well as with standard laparoscopic instrumentation such as Kelly forceps, right angle forceps, and Ligasure. Ventral compartment exploration, dorsal compartment exploration, and lymph node extirpation was unable to be successfully performed due to the limited field of view of the mediastinoscope, restriction of lateral and dorsoventral excursion of the instruments when passed through the working channel, inability to sufficiently stabilize the instruments for safe dissection when passed alongside (external to) the mediastinoscope, the functional mismatch in the depth of working distance within the canine mediastinum and short length of the mediastinoscopic-specific instruments, and lack of trocar constraint/provided pivot point for the longer standard laparoscopic instruments that resulted in a loss of fine control at the level of dissection. This technique was subsequently abandoned without further data collection.

Alternative VAMLA (aVAMLA) – an alternative VAMLA technique was conceived utilizing a SILS port, and this procedure was subsequently performed in nine cadavers. The first two cadavers were utilized to optimize procedural technique and specific data was not recorded. Data collection was subsequently performed on the remaining seven cadavers.

## 3.2 | Preprocedure thoracic CT

CT-measured cranial mediastinal dimensions are reported in Table 1. CT-imaging identification of the right and left sternal lymph nodes (STLN), left, right, and middle tracheobronchial lymph nodes (TBLN), and variable cranial mediastinal lymph nodes are reported in Table 2. Median and ranges for lymph node width, height, length, and volume were also reported in Table 2. The vascular “sling”, defined as the brachycephalic venous arch, was identified on CT in all seven dogs, as well as the mediastinal pleura, carina, pulmonary arch, and the azygous vein. The internal thoracic vessels and thymus were identified in 6/7 dogs, and the recurrent laryngeal nerve was identified in 5/7 dogs. The esophagus was identified in 4/7 dogs, and the aortic arch was identified in 3/7 dogs.

## 3.3 | Post-procedure thoracic CT

Following aVAMLA, mediastinal gas was retained in all 7 cadavers and pleural gas was identified in 4/7

TABLE 1 Cranial mediastinal dimensions.

CrM CSA at site of maximal thymic size (cm <sup>2</sup> )	CrM volume (as % of thoracic cavity) at site of maximal thymic size	Volume of transverse plane at CrM at midpoint (cm <sup>3</sup> )	Distance from ventral neck at thoracic inlet to carina (cm)
24.2 (range 23.6–28)	80.4 (61.2–100)	6.6 (2.7–9)	17.3 (15.1–18.3)

Abbreviations: CrM, cranial mediastinum; CSA, calculated surface area.

TABLE 2 Thoracic CT identification and size/volume measurements of cranial mediastinal, sternal, and tracheobronchial lymph nodes.

Lymph node	Rate of identification (no. of cadavers)	Width, cm, median (range)	Height, cm, median (range)	Length, cm, median (range)	Volume, cm <sup>3</sup> median (range)
RSTLN	7/7	0.6 (0.4–0.7)	0.6 (0.5–0.9)	1.4 (0.9–3.1)	1.5 (0.9–6.2)
LSTLN	6/7	0.5 (0.3–0.8)	0.6 (0.3–1.2)	1.2 (0.5–1.3)	1.5 (0.2–6.8)
RTBLN	5/7	0.8 (0.2–0.9)	0.6 (0.3–1.4)	0.5 (0.4–0.8)	1.1 (0.2–2.6)
LTBLN	7/7	1 (0.3–2)	0.7 (0.5–1.2)	1.2 (0.5–2.4)	4.5 (0.5–15.2)
Middle TBLN	7/7	0.6 (0.3–1.2)	0.6 (0.4–1.1)	0.6 (4–24)	1.2 (0.3–1.3)
Cranial mediastinal LN	7/7 <sup>a</sup>	0.6 (0.4–1.1)	0.8 (0.4–1.4)	1.1 (0.4–2.5)	1.9 (0.5–15.8)

Abbreviations: CT, computed tomography; LN, lymph node; LSTLN, left sternal lymph node; LTBLN, left tracheobronchial lymph node; RSTLN, right sternal lymph node; RTBLN, right tracheobronchial lymph node; TBLN, tracheobronchial lymph node.

<sup>a</sup>Single LN in 5/7, two in 2/7.

TABLE 3 Quantification of mediastinal and pleural gas.

CrM gas (% of total thoracic cavity CSA between second and third ribs)	CrM gas (% of total thoracic cavity CSA between manubrium and second sternal segment)	Pleural gas (% of total thoracic CSA at level of the mid-heart)
4.5 (0–25.5)	27.7 (5.6–40.1)	(4.2 (0–50))

Abbreviations: CrM, cranial mediastinum; CSA, calculated surface area.

cadavers. Quantification of mediastinal and pleural gas is described in Table 3.

Post-procedural subcutaneous gas was limited to the port insertion location in 6/7 cadavers, but in 1/7 cadavers gas dissected subcutaneously along the left axilla and thoracic wall. Intermuscular gas was limited cranially to the level of C3 in 6/7 cadavers and invaded more deeply into the muscles lining the thoracic wall in the region of the axilla in 1/7.

### 3.4 | aVAMLA procedure

The SILS port and associated cannula placement took a median of 5 min (range, 5–10). The initial dissection plane along the ventral surface of the trachea was established via finger dissection and use of a blunt trocar in 6/7 cadavers, and with finger dissection alone in 1/7. With a longer reach than obtained by a finger alone, use

of the blunt trocar to aid development of this potential space provided subjectively improved initial working space and visualization. The preferred camera port position was the upper left port within the 3-port SILS system in 7/7 cadavers, and instruments used during the procedure included a blunt laparoscopic probe (2/7 cadavers), laparoscopic right-angle dissectors (7/7), laparoscopic straight Kelly dissectors (7/7) and a 5 mm LigaSure Dolphin handpiece (7/7). Dissection time from the thoracic inlet to the carina was recorded as a median of 7 min (range, 3–33 min). Ventral compartment exploration time was a median of 27 min (range, 7–49 min). The relevant surgical anatomy of both mediastinal compartments is demonstrated in Figure 3. Structures visualized included the arch of the brachycephalic veins (in 7/7 cadavers), the sternum (7/7), left internal thoracic vein/artery (6/7), right internal thoracic vein/artery (6/7), the thymus gland (5/7), and the lateral mediastinal pleura (7/7). In all five cadavers for which the thymus was noted, visualization of remaining structures within the ventral compartment was compromised.

Dorsal compartment exploration time was a median of 30 min (range, 15–55 min). Structures visualized included the carina (7/7 cadavers), pulmonary trunk (7/7), azygous vein (7/7), recurrent laryngeal nerve (5/7), esophagus (4/7), and the aortic arch (3/7). The median weighted NASA-TLX score for dorsal compartment and ventral compartment exploration and assessment was 27 (range, 20–49) and 74.3 (range, 62.3–96.3), respectively.

TABLE 4 Identification and retrieval of cranial mediastinal lymph nodes.

Lymph node	Identified on CT scan (no. cadavers)	Volume, cm <sup>3</sup> median (range)	Identified on mediastinoscopy (no. cadavers)	Retrieved with mediastinoscopy (no. cadavers)	Dissection Time, min median (range)	Procedure visualization score median (range)	Procedure dissection/retrieval score median (range)	Weighted NASA-TLX median (range)
LTBLN	7/7	4.5 (.5–15.2)	7/7	7/7	13 (9–23)	2 (1–2)	2 (2–3)	62 (38–69)
RTBLN	5/7	1.1 (0.2–2.6)	5/7	4/7	4 (2–9)	3 (1–5)	4 (1–5)	35 (14–87)
Right sternal	7/7	1.5 (0.9–6.2)	3/7	3/7	10 (8–32)	5 (3–5)	4 (3–5)	84 (70–98)
Left sternal	6/7	1.5 (0.2–6.8)	2/7	2/7	2, 14	5 (3–5)	5 (3–5)	97 (74–98)
Cranial mediastinal	7/7	1.9 (0.5–15.8)	1/7	1/7	5	5 (1–5)	5 (1–5)	44

Abbreviations: CT, computed tomography; LTBLN, left tracheobronchial lymph node; RTBLN, right tracheobronchial lymph node; TBLN, tracheobronchial lymph node.

Procedural data regarding the rate of visualization and successful retrieval of different lymph nodes is reported in Table 4. Median and ranges for dissection times in minutes, weighted NASA-TLX per lymph node extirpation, and procedure success score for visualization and tissue extirpation were reported in Table 4. In all cases, authors considered all visualized lymph nodes to be amenable to biopsy by cup forceps even if unable to be fully extirpated via the described approach.

Recorded adverse operative events included a grade 1 iatrogenic tissue injury in 2/7 cadavers (torn LTBLN in one, pleural rupture in one). Accumulation of surgical smoke in the small working space during deployment of the LigaSure device was defined as a grade 1 technical failure due to impeded visualization and dissection. This occurred in 7/7 cadavers.

## 4 | DISCUSSION

The alternative VAMLA approach using a SILS port and standard laparoscopic instrumentation was found to be technically feasible for the retrieval of normal lymph nodes in adult canine cadavers. While an initial attempt using a commercial mediastinoscopic system designed for humans was made, this instrumentation did not adapt well to the canine thoracic anatomy.

Utility of the mediastinoscope for sVAMLA within the canine cadaveric cranial mediastinum was found to be poor. While the authors acknowledge that limitations of the video mediastinoscope may have been anticipated based on known dimensions of the canine cranial mediastinum, attempts at using this device found the working space provided by the mediastinoscope did not translate functionally to canine mediastinum. The mediastinoscopy-specific instruments designed to be used within the mediastinoscope working channel were too short to reach the structures of interest within the canine mediastinum, requiring use of longer laparoscopic instruments. Additionally, the working channel of the mediastinoscope was long (20 cm) and limited lateral and dorsoventral motion of the instruments. The smooth metal working channel provided very little fixed contact with the instruments, which made the standard long laparoscopic instruments difficult to use safely and effectively. While tissue retraction from the mediastinoscope was advantageous, the SILS port provided a fixed fulcrum which enabled stability and operator-directed lateral and dorsoventral instrument excursions.

Suggested contraindications for this mediastinoscopy in people include patients with coagulopathies, severe cerebrovascular disease, bulky disease, or extranodal tumor growth.<sup>29–31</sup> Obesity, while not linked to poor

surgical outcomes in minimally invasive surgery in people,<sup>32</sup> could be a limitation in the successful application of this technique due to the presumed negative effects of increased mediastinal fat on structure visualization and further reduction of working space in this limited access area and more distant location of the relevant lymph nodes within the thorax from the approach site than in humans. Additionally, the authors only encountered normal lymph nodes and larger nodes may pose challenges. Importantly, all visualized lymph nodes in the studied cohort were subjectively considered able to be safely biopsied using a laparoscopic cup biopsy forceps instrument, and so some benefit may still exist in this approach for incisional sampling of moderately to severely enlarged lymph nodes in the canine cranial mediastinum. The impacts of cardiac and respiratory motion and ventilation tidal volume were not assessed in this cadaveric study and might also impact the success of this procedure in live animals.

The thoracic CT scan performed did not utilize an intravenous contrast agent, although mediastinal adipose provided tissue contrast and enabled lymph node identification and measurement.<sup>33</sup> There was moderate difficulty in identifying all lymph nodes that were found on thoracic CT scan with aVAMLA (Table 4). The most consistently visualized on thoracic CT and retrieved with aVAMLA were the right and left tracheobronchial lymph nodes. This is likely related to their position directly adjacent to the identifiable structures of the right and left bronchus, respectively and the relative ease of following the trachea directly to this area. The overall low NASA-TLX scores of lymph node retrieval for RTBLN and LTBLN mirrored the successful retrieval of these lymph nodes in most cadavers. The sternal and cranial mediastinal lymph nodes were frequently obscured by the presence of the thymus and mediastinal fat. Interestingly, the only retrieved cranial mediastinal lymph node had a relatively low NASA-TLX score, suggesting that these lymph nodes might be retrieved easily once identified, which may be more straightforward in live dogs. The addition of contrast lymphangiography or disease infiltration within lymph nodes of interest may enable easier identification and improve the rate of retrieval in clinical cases.

Described complications of sVAMLA in people include temporary left recurrent nerve paralysis most commonly, as well as hemorrhage, pleural effusion, chylothorax, and mediastinitis, with an overall complication rate of 2.6%–11.3%.<sup>19–22,29</sup> While the recurrent laryngeal nerve was consistently identified and functional assessment was impossible in this cadaveric cohort, nerve injury remains a relevant concern. The optimal plane of dissection was identified within the paratracheal fascia at the ventral aspect of the trachea. Thermal spread from

the LigaSure and attenuation of blood supply within this dissection plane may lead to tracheal injury although this is considered unlikely.<sup>34,35</sup> Finally, while no vascular disruption was observed within this cohort, the proximity of essential blood vessels makes this an important potential ramification.

Mild mediastinal insufflation was used in this technique, with a maximal pressure of 4 mmHg, based on prior studies suggesting that pleural pressure of up to 5 mmHg during thoracoscopy may be tolerated.<sup>36,37</sup> The addition of insufflation provided appreciable support in defining the potential space and improvement in visualization. Presence of mild post-procedure pleural gas most likely a result of leakage of insufflation gas from the mediastinum from secondary disruption to the pleura that was difficult to appreciate. The clinical significance of this is unknown, although transient loss in mediastinal space pressure leading to collapse of working space could be experienced which could prolong the procedure.

The SILS port was introduced cranial to the level of the thoracic inlet, along the ventral aspect of the neck, with an incision size that varied from 3 to 5 cm. The authors found that seating the cuff of the SILS port between the ventral musculature of the neck and deep to the level of the paratracheal fascia enabled immediate access to important landmarks. There was notable retention of smoke following deployment of the LigaSure device during lymphadenectomy at all sites, in all cadavers. This should be anticipated due to the small working space and lack of ventilation. Surgical smoke is known to inhibit visualization and identifying safe and effective solutions for image enhancement<sup>38</sup> and smoke evacuation<sup>39,40</sup> have been pursued. Future investigations of this procedure include considering smoke evacuation systems compatible with the SILS system such as the AirSeal device or homemade cannula alterations.<sup>40,41</sup>

This study had several important limitations. The limited experience in a small cohort of seven large breed canine cadavers, previously frozen and thawed, may have prevented the investigators in fully understanding the challenges of aVAMLA. Translation of this technique in clinical cases of variably sized dogs including small breed dogs, with diseased lymph nodes may be challenging and important clinical consequences and the complication likelihood in live patients may be under-appreciated. However, lymph node identification can be difficult in cadaveric tissue, and may be easier in living dogs. Additionally, the sVAMLA was only attempted to be used in one cadaver and progressive utility may have been gained by further attempts. In addition to lymphadenectomy, it should be considered that access to the cranial mediastinum may allow for retrieval of small and non-invasive cranial mediastinal masses, which has been




successfully although infrequently reported in the human literature, but this was not evaluated in this cohort.<sup>42–44</sup>

In conclusion, this study suggests that aVAMLA is technically feasible and can be successful in identifying and retrieving and/or obtaining biopsies of mediastinal lymph nodes in large breed canine cadaver specimens. Staging of mediastinal lymph nodes is challenging, currently commonly requiring open surgical retrieval, but yet is an important piece in the decision making for treatment of intrathoracic neoplasms in dogs.<sup>1–10</sup> Providing minimally invasive alternatives to transthoracic extirpation of these lymph nodes in clinical cases may allow maximization of patient outcomes. Assessment in a live dog model is recommended prior to considering aVAMLA in clinical cases requiring cranial mediastinal mass resection or lymph node staging.

### CONFLICT OF INTEREST STATEMENT

The authors declare no conflicts of interest related to this report.

### ORCID

Michele A. Steffey  <https://orcid.org/0000-0003-0852-0644>

### REFERENCES

- Moore EL, Vernau W, Rebhun RB, Skorupski KA, Burton JH. Patient characteristics, prognostic factors and outcome of dogs with high-grade primary mediastinal lymphoma. *Vet Comp Oncol.* 2018;16(1):E45–E51.
- Liptak JM, Kamstock DA, Dernell WS, Ehrhart EJ, Rizzo SA, Withrow SJ. Cranial mediastinal carcinomas in nine dogs. *Vet Comp Oncol.* 2008;6(1):19–30.
- Robat CS, Cesario L, Gaeta R, Miller M, Schrempp D, Chun R. Clinical features, treatment options, and outcome in dogs with thymoma: 116 cases (1999–2010). *J Am Vet Med Assoc.* 2013;243(10):1448–1454.
- McPhetridge JB, Scharf VF, Regier PJ, et al. Distribution of histopathologic types of primary pulmonary neoplasia in dogs and outcome of affected dogs: 340 cases (2010–2019). *J Am Vet Med Assoc.* 2021;260(2):234–243.
- Rose RJ, Worley DR. A contemporary retrospective study of survival in dogs with primary lung tumors: 40 cases (2005–2017). *Front Vet Sci.* 2020;7:519703.
- McNiel EA, Ogilvie GK, Powers BE, Hutchison JM, Salman MD, Withrow SJ. Evaluation of prognostic factors for dogs with primary lung tumors: 67 cases (1985–1992). *J Am Vet Med Assoc.* 1997;211(11):1422–1427.
- Ogilvie GK, Weigel RM, Haschek WM, et al. Prognostic factors for tumor remission and survival in dogs after surgery for primary lung tumor: 76 cases (1975–1985). *J Am Vet Med Assoc.* 1989;195(1):109–112.
- Polton GA, Brearley MJ, Powell SM, Burton CA. Impact of primary tumour stage on survival in dogs with solitary lung tumours. *J Small Anim Pract.* 2008;49(2):66–71.
- Lee BM, Clarke D, Watson M, Laver T. Retrospective evaluation of a modified human lung cancer stage classification in dogs with surgically excised primary pulmonary carcinomas. *Vet Comp Oncol.* 2020;18(4):590–598.
- Ichimata M, Kagawa Y, Namiki K, et al. Prognosis of primary pulmonary adenocarcinoma after surgical resection in small-breed dogs: 52 cases (2005–2021). *J Vet Intern Med.* 2023;37(4):1466–1474.
- Evans HE, Lahunta AD. *Miller's anatomy of the dog.* 4th ed. Elsevier; 2013.
- Tuohy JL, Worley DR. Pulmonary lymph node charting in normal dogs with blue dye and scintigraphic lymphatic mapping. *Res Vet Sci.* 2014;97(1):148–155.
- Steffey MA, Daniel L, Mayhew PD, Affolter VK, Soares JH, Smith A. Video-assisted thoracoscopic extirpation of the tracheobronchial lymph nodes in dogs. *Vet Surg.* 2015;44(Suppl 1):50–58.
- Suga K, Yuan Y, Ueda K, et al. Computed tomography lymphography with intrapulmonary injection of iopamidol for sentinel lymph node localization. *Invest Radiol.* 2004;39(6):313–324.
- Paoloni MC, Adams WM, Dubielzig RR, Kurzman I, Vail DM, Hardie RJ. Comparison of results of computed tomography and radiography with histopathologic findings in tracheobronchial lymph nodes in dogs with primary lung tumors: 14 cases (1999–2002) [published correction appears in *J Am vet med Assoc.* 2006 Sep 1;229(5):710]. *J Am Vet Med Assoc.* 2006;228(11):1718–1722.
- Reich JM, Brouns MC, O'Connor EA, Edwards MJ. Mediastinoscopy in patients with presumptive stage I sarcoidosis: a risk/benefit, cost/benefit analysis. *Chest.* 1998;113(1):147–153.
- Mineo TC, Ambrogi V, Nofroni I, Pistolesse C. Mediastinoscopy in superior vena cava obstruction: analysis of 80 consecutive patients. *Ann Thorac Surg.* 1999;68(1):223–226.
- Carlens E. Mediastinoscopy: a method for inspection and tissue biopsy in the superior mediastinum. *Dis Chest.* 1959;36:343–352.
- Leschber G, Holinka G, Linder A. Video-assisted mediastinoscopic lymphadenectomy (VAMLA) – a method for systematic mediastinal lymphnode dissection. *Eur J Cardiothorac Surg.* 2003;24(2):192–195.
- Witte B, Hürtgen M. Video-assisted mediastinoscopic lymphadenectomy (VAMLA). *J Thorac Oncol.* 2007;2(4):367–369.
- Witte B, Wolf M, Huertgen M, Toomes H. Video-assisted mediastinoscopic surgery: clinical feasibility and accuracy of mediastinal lymph node staging. *Ann Thorac Surg.* 2006;82(5):1821–1827.
- Call S, Obiols C, Rami-Porta R, et al. Video-assisted mediastinoscopic lymphadenectomy for staging non-small cell lung cancer. *Ann Thorac Surg.* 2016;101(4):1326–1333.
- Hartert M, Tripsky J, Huertgen M. Video-assisted mediastinoscopic lymphadenectomy (VAMLA) for staging & treatment of non-small cell lung cancer (NSCLC). *Mediastinum.* 2020;4:3.
- El-Sherief AH, Lau CT, Wu CC, Drake RL, Abbott GF, Rice TW. International association for the study of lung cancer (IASLC) lymph node map: radiologic review with CT illustration. *Radiographics.* 2014;34(6):1680–1691.
- Rusch VW, Asamura H, Watanabe H, et al. The IASLC lung cancer staging project: a proposal for a new international

- lymph node map in the forthcoming seventh edition of the TNM classification for lung cancer. *J Thorac Oncol*. 2009;4(5):568-577.
26. Follette CM, Giuffrida MA, Balsa IM, et al. A systematic review of criteria used to report complications in soft tissue and oncologic surgical clinical research studies in dogs and cats. *Vet Surg*. 2020;49:61-69.
  27. Balsa IM, Giuffrida MA, Mayhew PD. A randomized controlled trial of three-dimensional versus two-dimensional imaging system on duration of surgery and mental workload for laparoscopic gastropexies in dogs. *Vet Surg*. 2021;50(5):944-953.
  28. Lowndes BR, Forsyth KL, Blocker RC, et al. NASA-TLX assessment of surgeon workload variation across specialties. *Ann Surg*. 2020;271(4):686-692.
  29. Park BJ, Flores R, Downey RJ, Bains MS, Rusch VW. Management of major hemorrhage during mediastinoscopy. *J Thorac Cardiovasc Surg*. 2003;126(3):726-731.
  30. Witte B, Hürtgen M. Video-assisted mediastinoscopic lymphadenectomy. *Multimed Man Cardiothorac Surg*. 2007;2007(1018):mmcts.2006.002576.
  31. Zieliński M. Transcervical extended mediastinal lymphadenectomy: results of staging in two hundred fifty-six patients with non-small cell lung cancer. *J Thorac Oncol*. 2007;2(4):370-372.
  32. Curet MJ. Special problems in laparoscopic surgery. Previous abdominal surgery, obesity, and pregnancy. *Surg Clin North Am*. 2000;80(4):1093-1110.
  33. Kayanuma H, Yamada K, Maruo T, Kanai E. Computed tomography of thoracic lymph nodes in 100 dogs with no abnormalities in the dominated area. *J Vet Med Sci*. 2020;82(3):279-285.
  34. Bercic J, Pocajt M, Drzecnik J. The influence of tracheal vascularization on the optimum location, shape and size of the tracheostomy in prolonged intubation. *Resuscitation*. 1978;6(2):131-143.
  35. Rosati T, Burkitt JM, Watson KD, et al. Obstructive tracheal necrosis in a dog secondary to smoke inhalation injury—case report. *Front Vet Sci*. 2020;7:409.
  36. Kanai E, Matsutani N, Watanabe R, et al. Effects of combined one-lung ventilation and intrathoracic carbon dioxide insufflation on intrathoracic working space when performing thoracoscopy in dogs. *Am J Vet Res*. 2022;83(9).
  37. Daly CM, Swalec-Tobias K, Tobias AH, Ehrhart N. Cardiopulmonary effects of intrathoracic insufflation in dogs. *J Am Anim Hosp Assoc*. 2002;38(6):515-520.
  38. Wang C, Alaya Cheikh F, Kaaniche M, Beghdadi A, Elle OJ. Variational based smoke removal in laparoscopic images. *Biomed Eng Online*. 2018;17(1):139.
  39. Takahashi H, Yamasaki M, Hirota M, et al. Automatic smoke evacuation in laparoscopic surgery: a simplified method for objective evaluation. *Surg Endosc*. 2013;27(8):2980-2987.
  40. Greaves N, Nicholson J. Single incision laparoscopic surgery in general surgery: a review. *Ann R Coll Surg Engl*. 2011;93(6):437-440.
  41. Bracale U, Silvestri V, Pontecorvi E, et al. Smoke evacuation during laparoscopic surgery: a problem beyond the COVID-19 period. A quantitative analysis of CO<sub>2</sub> environmental dispersion using different devices. *Surg Innov*. 2022;29(2):154-159.
  42. McNally PA, Arthur ME. *Mediastinoscopy*. StatPearls Publishing; 2022 Accessed December 12, 2022.
  43. Uchiyama A, Shimizu S, Murai H, Kuroki S, Okido M, Tanaka M. Infrasternal mediastinoscopic thymectomy in myasthenia gravis: surgical results in 23 patients. *Ann Thorac Surg*. 2001;72(6):1902-1905.
  44. Klingen G, Johansson L, Westerholm CJ, Sundstroöm C. Transcervical thymectomy with the aid of mediastinoscopy for myasthenia gravis: eight years' experience. *Ann Thorac Surg*. 1977;23(4):342-347.

## SUPPORTING INFORMATION

Additional supporting information can be found online in the Supporting Information section at the end of this article.

**How to cite this article:** Gibson EA, Brust K, Steffey MA. Evaluation of mediastinoscopy for cranial mediastinal and tracheobronchial lymphadenectomy in canine cadavers. *Veterinary Surgery*. 2024;53(5):834-843. doi:10.1111/vsu.14095